reaction is a fraction of the energy gap at the reactant end, and it takes the general form $E^* = r(I_{N:} - A_{CH_3X}) - |\beta|$. *r* is a factor which depends on the slopes of descent and the type of the two intersecting curves. This equation can be applied to thermoneutral as well as to exothermic (and endothermic) reactions, and thus it compliments both the Marcus equation and the BEP principle.

The slopes of descent of the intersecting curves are influenced, amongst other factors, by (a) the amount of delocalization (strength) of the 3-electron bonds $(C.\cdot.X)^-$ and $(C.\cdot.N)^-$, (b) specific localization requirements, e.g., in CH$_3$–H (eq 27) or in CF$_3$CO$_2^-$, NC$^-$ (eq 28), and (c) the C–X and N–C bond strength difference. As the 3-electron bonds become stronger and the localization requirement more severe, the descent of the curves is retarded and a larger fraction of the gap $(I_{N:} - A_{CH_3X})$ enters the activation barrier (*r* is large). On the other hand, as the 2-electron bond strength (N–C vs. C–X) differences increase, a smaller fraction of the gap enters the activation barrier.

Thus, in general the ensemble of S$_N$2 reaction will exhibit (a) *electron-transfer-controlled* reactivity patterns which obey the donor–acceptor (or gap $I_{N:} - A_{CH_3X}$) abilities of the reactants[29] and (b) *slope-controlled reactivity patterns which respond* to the strengths of the 3-electron bonds, localization effects, etc. An important conclusion is that improving the donor–acceptor abilities of the reactants does not guarantee high S$_N$2 reactivity if at the same time this improvement creates severe localization demands. An example is the sluggish S$_N$2 reactivities of the good electron acceptors CCl$_4$ and CH$_2$Cl$_2$[44] in comparison with the poorer acceptor CH$_3$Cl. However, since the position of crossing ("late" vs. "early") depends on the donor–acceptor abilities (the gap $I_{N:} - A_{RX}$),[4b,46] their significant improvement is likely to lead to bona fide electron-transfer reactions, especially if such an improvement also creates specific localization requirements (e.g., in CCl$_4$)[47] which now takes place after crossing occurs.

Strong 3-electron bonds and specific localization requirements are also the cause for the breakdown of the universality of the BEP principle. The BEP principle is shown to apply with certainty only when an increase in reaction exothermicity does not involve significant changes in these factors.

In the future we hope to consider the effect of solvent on the barrier height as well as the concepts of nucleophilicity and leavhing group ability using eq 32.

Acknowledgment. We are indebted to Dr. S. Efrima for helpful suggestions and Professor J. F. Bunnett for stimulating discussions. S.S.S. thanks Dr. H. Köppel for very enlightening discussions on curve crossing.

Registry No. F, 16984-48-8; Cl, 16887-00-6; Br, 24959-67-9; I, 20461-54-5; HO, 14280-30-9; CH$_3$O, 3315-60-4; CF$_3$CO$_2$, 14477-72-6; CH$_3$S, 17302-63-5; NC, 57-12-5; HCC, 29075-95-4; H, 12184-88-2; H$_2$N, 17655-31-1; CH$_3$F, 593-53-3; CH$_3$Cl, 74-87-3; CH$_3$Br, 74-83-9; CH$_3$I, 74-88-4; CF$_3$CO$_2$CH$_3$, 431-47-0; CH$_3$OH, 67-56-1; CH$_3$OCH$_3$, 115-10-6; CH$_3$SCH$_3$, 75-18-3; N≡CCH$_3$, 75-05-8; HC≡CCH$_3$, 74-99-7; CH$_4$, 74-82-8; H$_2$NCH$_3$, 74-89-5; CH$_3$F radical anion, 34475-43-9; CH$_3$Cl radical anion, 69685-01-4; CH$_3$Br radical anion, 40431-10-5; CH$_3$I radical anion, 40431-11-6; CH$_3$OH radical anion, 68474-04-4; CH$_3$OCH$_3$ radical anion, 81132-07-2; CF$_3$CO$_2$CH$_3$ radical anion, 81096-78-8; CH$_3$SCH$_3$ radical anion, 70332-64-8; NCCH$_3$ radical anion, 28486-62-6; HC≡CCH$_3$ radical anion, 81132-08-3; CH$_4$ radical anion, 27680-53-1; H$_2$NCH$_3$ radical anion, 81096-79-9.

---

(46) Using eq 25 and 24 it is possible to show that the position of the intersection point (Q_c) is $Q_c = (I_{N:} - A_{RX})/k$. This means that when $I_{N:} - A_{RX}$ approaches zero, the crossing point approaches the reactant (r) position, $Q_r = 0$.

(47) See, for example: (a) Meyers, C. Y.; Kolb, V. M. *J. Org. Chem.* **1978**, *43*, 1985–1990. (b) Ashby, E. C.; Goel, A. B.; Depriest, R. N. *J. Org. Chem.* **1981**, *46*, 2431–2433. (c) Ashby, E. C.; Goel, A. B.; DePriest, R. N. *J. Am. Chem. Soc.* **1980**, *102*, 7779. (d) Ashby, E. C.; Goel, A. B.; DePriest, R. N.; Prasad, H. S. *Ibid.* **1981**, *103*, 973. (e) Ashby, E. C.; DePriest, R. N.; Goel, A. N. *Tetrahedron Lett.* **1981**, *22*, 1763–1766.

Ab Initio Studies of the Structures of Peroxides and Peroxy Radicals

Raymond A. Bair[†] and William A. Goddard III*

Contribution No. 6508 from the Arthur Amos Noyes Laboratory of Chemical Physics, California Institute of Technology, Pasadena, California 91125. Received August 14, 1981

Abstract: Ab initio theoretical calculations of the equilibrium structures of CH$_3$OOCH$_3$, CH$_3$OOH, HOOH, CH$_3$OO·, and HOO· are compared. The wave functions are calculated by using generalized valence bond (GVB) and configuration interaction methods. It is found that CH$_3$OOCH$_3$ is trans (planar), while CH$_3$OOH and HOOH exhibit dihedral angles of 126° and 119°, respectively. The theoretically determined structures of HOOH and HOO· agree closely with the accepted experimental structures. For the remaining species, very few experimental structural parameters are available.

Alkyl peroxides play an important part in hydrocarbon oxidation processes, yet few structural data are available, and reliable theoretical studies have previously been limited to the hydroperoxy species. In this study we have carried out ab initio generalized valence bond (GVB) and configuration interaction (CI) studies of the structures of the hydroperoxides, methyl peroxides, and the corresponding peroxy radicals:

$$HOOH, \ CH_3OOH, \ CH_3OOCH_3, \ HOO\cdot, \ CH_3OO\cdot$$
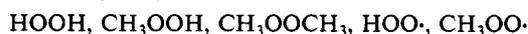
In all of these species it is necessary to include electron correlation

Table I. Equilibrium Structure of CH$_3$O·

	r_{CO}	r_{CH_a}	r_{CH_s}	θ_{OCH_a}	θ_{OCH_s}
GVB + CI	1.410	1.112	1.111	111.1	106.9
exptl[a] (CH$_3$OCH$_3$)	1.410	1.100	1.091	110.8	107.2

in the wave function to determine an accurate equilibrium structure. Our calculations agree closely with the well-established experimental structures for HOOH and HOO·, giving strong support to the reliability of calculated structures for the remaining species.

---

†Chemistry Division, Argonne National Laboratory, Argonne, IL 60439

2720 *J. Am. Chem. Soc., Vol. 104, No. 10, 1982*

Bair and Goddard

Table II. Theoretical and Experimental Equilibrium Geometries of Peroxides[a]

method	r_{OO}	r_{OH}	r_{OC}	θ_{OOH}	θ_{OOC}	ϕ	ref
				A. HOOH			
exptl	1.463	0.967		99.3		120.2	5
ab initio							
correlated (GVB + CI)	1.464	0.967		99.9		119.1	this work
correlated (RS-MP2)	1.451	0.967		99.3		119.3	6
uncorrelated (RHF)	1.390	0.943		102.9		111.2	6
semiempirical							
MINDO/2	1.404	0.966		90.3		115.5	7
INDO	1.22	1.04		83.5		108.8	8
				B. CH₃OOH			
ab initio							
correlated (GVB + CI)	1.452	0.967	1.446	99.6	105.0	126	this work
semiempirical							
MINDO/2	1.414	0.970	1.338	115.6	119.0		7
CNDO/2	1.23	(0.96)	(1.44)	109	109		9
				C. CH₃OOCH₃			
exptl					105	~170[b]	11,13
ab initio							
correlated (GVB + CI)	1.450		1.444		104.1	180.0	this work
semiempirical							
MINDO/2	1.424		1.338		118.7	96.5	7

[a] Values in parentheses were assumed in the calculations. Distances are in angstroms and angles in degrees. ϕ is the dihedral angle. [b] See text.

Calculational Details

For carbon and oxygen, the (9s,5p) Gaussian basis of Huzinaga[1] was contracted by using Dunning's coefficients to the valence double-ζ (3s,2p) level.[2] In addition, d polarization functions (α = 0.99) were added to the oxygen atoms. The hydrogen basis consisted of the Huzinaga (5s) Gaussian basis contracted to three functions (but no scaled). Wherever hydrogen was bonded to oxygen, p polarization functions were added to the hydrogen (α = 1.25). This was found unnecessary for hydrogens bonded to carbon.

The C–H bond distances and O–C–H angles were chosen as those from the experimentally determined structure of dimethyl ether and not varied in our calculations. There is good support for this assumption since full optimization of the structure of $CH_3O\cdot$ led to essentially the same parameters (Table I). One would expect the methoxy radical to have larger C–H and O–C–H distortions than the other molecules in this study. Thus, in this study we optimized all the structural parameters for each molecule, except the C–H bond distances and O–C–H bond angles.

For each molecule the wave functions were solved self-consistently by using the GVB2.5 program.[3] All of the valence electrons in the C–O, O–O, and H–O bonds were correlated (GVB pairs), allowing each electron to have its own optimized orbital. The oxygen lone pairs were also correlated as GVB pairs. For example, HOOH with its seven valence electron pairs was described with 14 localized GVB orbitals (and two core orbitals) optimized self-consistently. For $CH_3OO\cdot$ we correlated all nine valence electron pairs, including the C–H bonds. However, the results were not significantly affected by the correlation in the CH bonds, and consequently, the C–H bonds were not correlated in CH_3OOH and CH_3OOCH_3.

The basis for CI calculations consisted of all of the GVB orbitals (two per bond or lone pair correlated). For the radicals, the singly occupied orbital was included, along with an additional more diffuse p-like orbital projected from the virtual space and centered on the radical atom. Thus both HOOH and $HOO\cdot$ have a CI basis of 14 orbitals. The CI calculation consisted of all single and double excitations from the dominant configuration plus all closed-shell quadrupole excitations from the dominant configu-

ration, restricting the electrons to remain within their respective GVB pairs. Of course, the radicals always had at least one open shell.

Results

HOOH. The structure of HOOH has been the focus of numerous experiments; however, these experiments do not provide an unambiguous structure. This is because there are four structural parameters to determine but only three rotational constants for the microwave spectra. The geometry often quoted is

$$R_0(OH) = 0.950 \text{ Å} \quad R_0(OO) = 1.475 \text{ Å}$$
$$\theta(OOH) = 94.8° \quad \phi(\text{dihedral}) = 111°$$

which was obtained with the assumption that $R_{OH} = 0.950$ Å.[4] In 1979, Cremer and Christen[5] reanalyzed the existing microwave data and concluded that more reasonable structures result from the assumption that $R_0(OH) = 0.965$ or 0.967 Å. This leads to the following structures:

$$R_0(OH) = 0.965 \text{ Å} \quad R_0(OO) = 1.464 \text{ Å}$$
$$\theta = 99.4° \quad \phi = 121.6°$$

and

$$R_0(OH) = 0.967 \text{ Å} \quad R_0(OO) = 1.463 \text{ Å}$$
$$\theta = 99.4° \quad \phi = 120.2°$$

As indicated in Table II, this is in almost exact agreement with our results:

$$R_e(OH) = 0.967 \text{ Å} \quad R_e(OO) = 1.464 \text{ Å}$$
$$\theta(OOH) = 99.9° \quad \phi = 119.1°$$

Another set of ab initio correlated wave functions was calculated by Cremer (RS-MP2),[6] leading to geometries almost identical with ours except that the OO bond is 0.01 Å shorter (1.451 Å). This may be due to some residual bias in the RS-MP2 approach due to starting with uncorrelated wave functions. Uncorrelated wave functions (RHF) lead to an error of –0.07 Å in the OO bond,

(1) S. Huzinaga, *J. Chem. Phys.*, **42**, 1293 (1965).
(2) T. H. Dunning, Jr. and P. J. Hay in "Methods of Electronic Structure Theory", H. F. Schaefer III, Ed.; Plenum Press: New York, 1977; p 23.
(3) GVB2.5 was written by R. A. Bair in 1977. This program is an extensively rearranged version of GVBTWO (written by F. W. Bobrowicz and W. R. Wadt in 1973) which avoids the extensive I/O requirements for cases with larger numbers of GVB pairs.

(4) R. L. Redington, W. B. Olson, and P. C. Cross, *J. Chem. Phys.*, **36**, 1311 (1962).
(5) D. Cremer and D. Christen, *J. Mol. Spectrosc.*, **74**, 480 (1979).
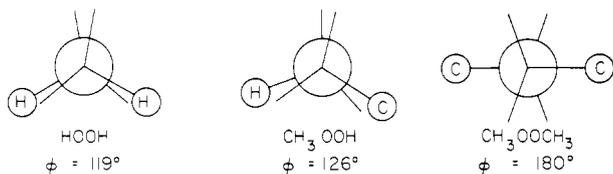(6) D. Cremer, *J. Chem. Phys.*, **69**, 4440 (1978).

Figure 1. Calculated equilibrium structures of peroxides, projected along the O–O bond. Lone pairs are shown as lines with no atoms at the terminus. In each case the angle between the two lone pairs on an oxygen is 140°.

–0.02-Å error in the OH bond, +3.5° in the OOH angle, and –9° in the dihedral angle.

The results from semiempirical and other approximate methods[7-10] lead to larger and nonsystematic errors, as indicated in Tables II and III. In general, MINDO/2 does fairly well for the bond distances of these species (except C–O bonds) but not very well for the bond angles, where errors of 10° or more are common. The INDO and CNDO/2 results are consistently poor. Our conclusion is that a proper description of electron correlation from ab initio calculations is essential to obtain accurate structural parameters.

CH₃OOH. No experimental structural data are available for methyl hydroperoxide, and to our knowledge, these calculations represent the first reported ab initio studies done on this molecule. Our calculated equilibrium structure is

$$R(OC) = 1.446 \text{ Å} \quad R(OH) = 0.967 \text{ Å} \quad R(OO) = 1.452 \text{ Å}$$

$$\theta(OOC) = 105.0° \quad \theta(OOH) = 99.6° \quad \phi = 126°$$

We observe that the calculated O–O length is 0.01 Å *shorter* than in hydrogen peroxide, in spite of the fact that thermochemical estimates would place the CH₃O–OH bond 5–10 kcal weaker. Hence, the O–O bond strengths do not correlate with the bond lengths for these peroxides.

On the other hand, the dihedral angle has increased from 119° in HOOH to 126° in CH₃OOH. The O–H bonds are polar, placing a small net positive charge on the hydrogen. Thus a small amount of stabilization can be gained by overlapping the hydrogens on one oxygen with the lone pairs on the other. In HOOH, the lowest energy conformation has each O–H bond nearly eclipsing a lone pair (Figure 1). In our calculations, the valence electrons are localized, so we are able to determine that the angle between the oxygen lone pairs on each oxygen is 140°. (The same angle is found for all three of the peroxides, while the angle is 123° in H₂O.) This makes the bond pair–lone pair angle 110°. Of course, the lone pairs on one oxygen will tend to repel those on the other, but there are two favorable hydrogen–lone pair interactions in HOOH and only one unfavorable interaction. Our calculations predict an inversion barrier of 1.0 kcal for HOOH, in excellent agreement with the value 1.1 kcal obtained from analysis of the near-infrared spectra.[11]

For CH₃OOH there is only one favorable interaction because the lone pair–methyl interaction is repulsive, opening the dihedral angle by 7°. Relative to previous theoretical studies (all semiempirical) of methyl hydroperoxide,[7,9] our OOC and OOH bond angles are significantly smaller. No previous estimate of the dihedral angle has been available. However, the zero-point energy in the torsional mode is greater than the calculated inversion barrier height (0.23 kcal), so considerable fluctuation is expected in this mode (Figure 2). Indeed, experiments may have difficulty in detecting the nonplanarity of the COOH group.
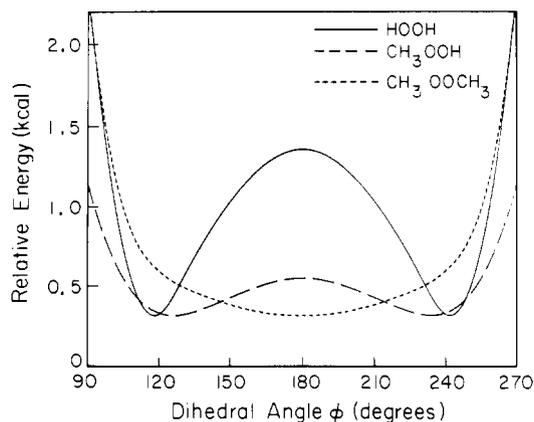
(7) K. Ohkubo, T. Fujita, and H. Sato, *J. Mol. Struct.*, **36**, 101 (1977).

(8) J. A. Pople and D. L. Beveridge, "Approximate Molecular Orbital Theory"; McGraw-Hill: New York, 1970; p 85.

(9) K. Ohkubo and F. Kitagawa, *Nippon Kagaku Kaishi*, 2147 (1973); *Bull. Chem. Soc. Jpn.*, **47**, 739 (1974).

(10) K. Ohkubo and F. Kitagawa, *Bull. Chem. Soc. Jpn.*, **48**, 703 (1975).

(11) R. H. Hunt, R. A. Leacock, C. W. Peters, and K. T. Hecht, *J. Chem. Phys.*, **42**, 1931 (1965).

Figure 2. Calculated potential curves as a function of dihedral angle. All other structural parameters are fixed at the calculated equilibrium values.
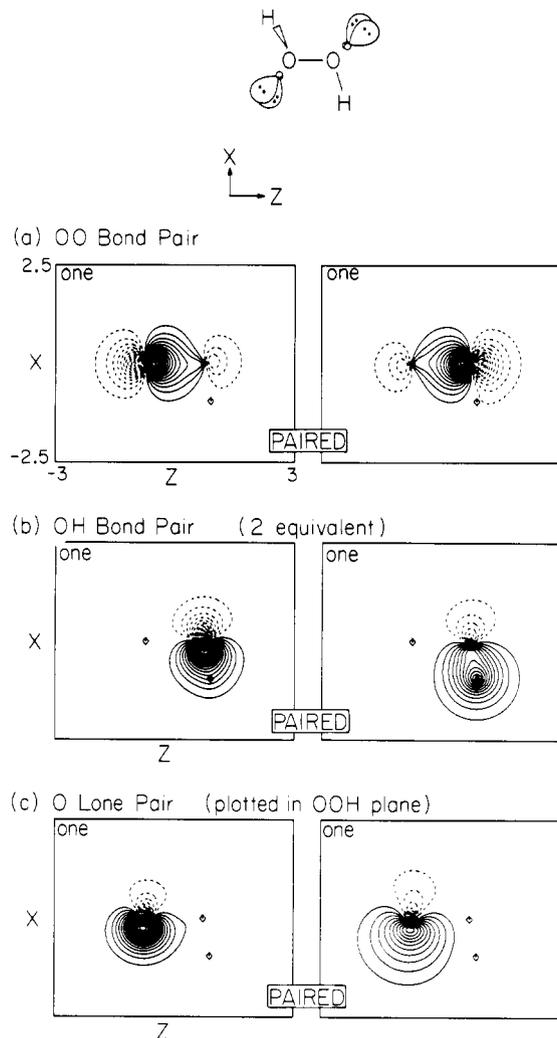

Figure 3. Orbital contour plots of the GVB orbitals of hydrogen peroxide. Solid lines indicate positive amplitude, and dashed lines indicate negative amplitude. The spacing between contours is 0.05 au. The same conventions are used for all plots. Note the interaction of the OH bond pair with the O lone pair nearly in the same plane.

CH₃OOCH₃. The O–O–C bond angle of dimethyl peroxide was obtained in 1950 from electron diffraction measurements.[12] Our calculated angle of 104.1° is well within the bounds of the ex-

(12) P. W. Allen and L. E. Sutton, *Acta Crystallogr.*, **3**, 46 (1950).

GVB ORBITALS OF CH_3OOH

(a) OO Bond Pair

(b) OC Bond Pair

(c) O Lone Pair

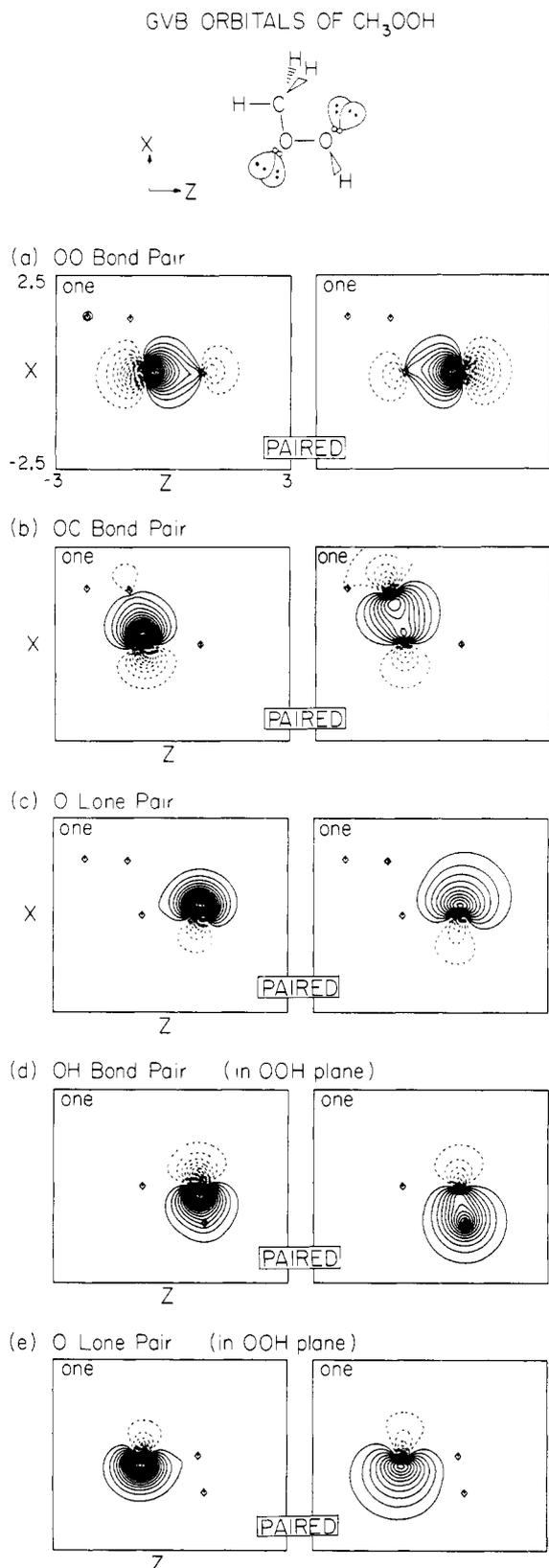(d) OH Bond Pair   (in OOH plane)

(e) O Lone Pair   (in OOH plane)

Figure 4. Contour plots of the GVB orbitals of CH_3OOH.

perimental value of 105 ± 3°. The electron diffraction data were not sufficient to determine the other structural parameters. The complete equilibrium structure calculated is

$$R(OC) = 1.444 \text{ Å} \qquad R(OO) = 1.450 \text{ Å}$$

$$\theta(OOC) = 104.1° \qquad \phi = 180°$$

Our calculated O–O bond distance of 1.450 Å is essentially the

Table III. Theoretical and Experimental Equilibrium Geometries of Peroxy Radicals[a]

method	r_{OO}	r_{OH}	r_{OC}	θ_{OOH}	θ_{OOC}	ref
		A. HOO				
exptl	1.335	0.977		104.1		14
ab initio correlated						
GVB + CI	1.342	0.972		104.2		this work
ab initio uncorrelated						
RHF	1.31	0.95		104		15
semiempirical						
MINDO/2	1.349	0.972		117.6		7
INDO	1.19	1.05		110.7		8
CNDO/2	1.19	(0.96)		111		9
		B. CH_3OO				
exptl						
ab initio correlated						
GVB + CI	1.339		1.442		110.2	this work
semiempirical						
MINDO/2	1.335		1.335		122.1	7
INDO	1.20		1.38		112.5	10
CNDO/2	1.19		(1.44)		111	9

[a] Values in parentheses were assumed in the calculations. Distances are in angstroms and angles in degrees.

GVB ORBITALS OF CH_3OOCH_3

(a) OO Bond Pair

(b) OC Bond Pair   (2 equivalent)
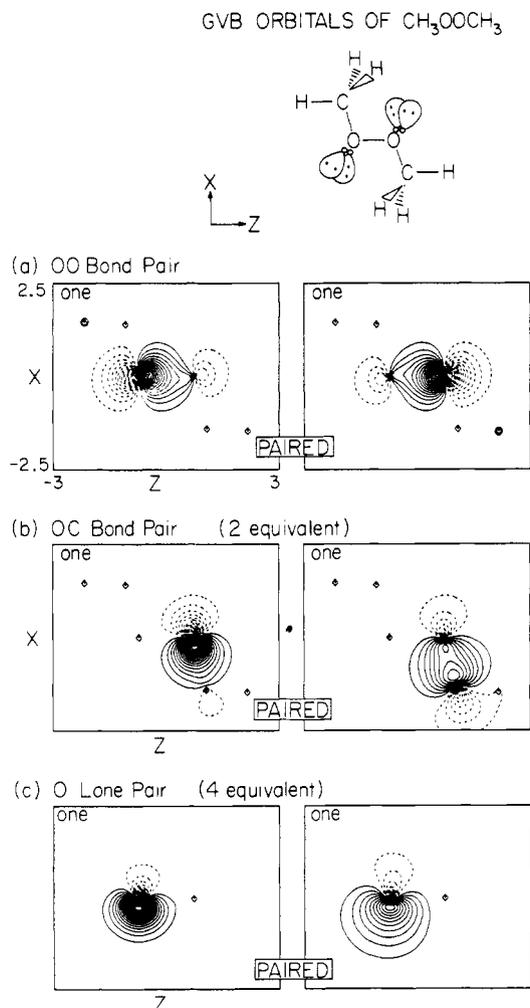
(c) O Lone Pair   (4 equivalent)

Figure 5. Contour plots of the GVB orbitals of CH_3OOCH_3.

same as that calculated for CH_3OOH (1.446 Å). Our calculated C–O bond length of 1.444 Å is 0.034 Å longer than is found experimentally for dimethyl ether.[13]

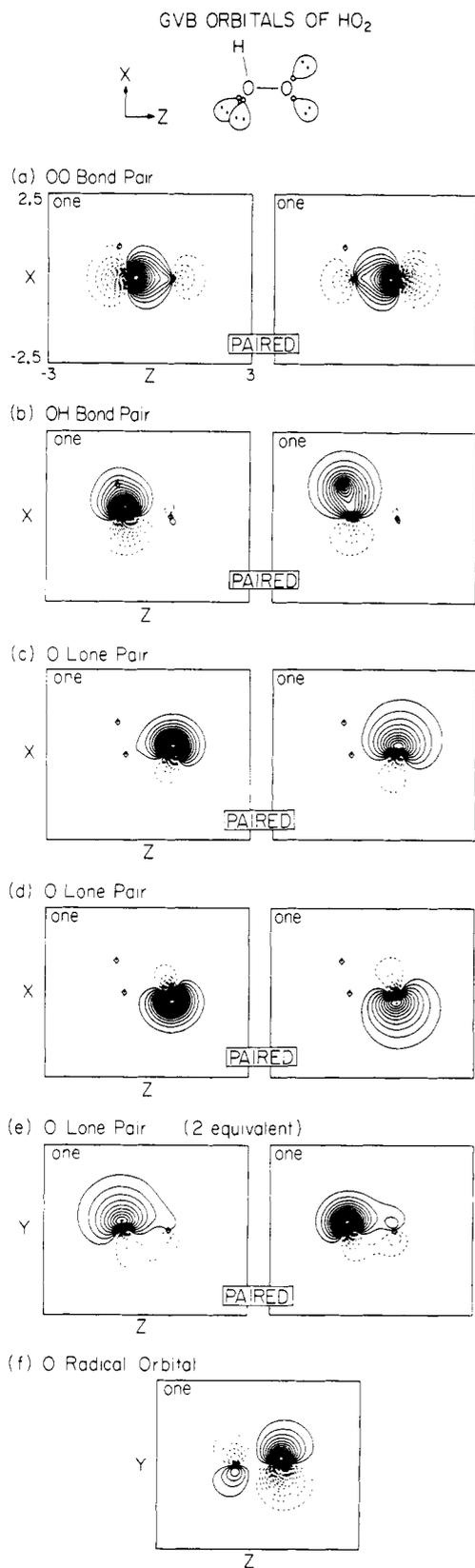(13) U. Blukis, P. H. Kasai, and R. J. Meyers, *J. Chem. Phys.*, **38**, 2753 (1963).

Structures of Peroxides and Peroxy Radicals

J. Am. Chem. Soc., Vol. 104, No. 10, 1982 2723

GVB ORBITALS OF HO₂

(a) OO Bond Pair

(b) OH Bond Pair

(c) O Lone Pair

(d) O Lone Pair

(e) O Lone Pair (2 equivalent)

(f) O Radical Orbital

Figure 6. Contour plots of the GVB orbitals of HO₂.

GVB ORBITALS OF CH₃O₂

(a) OC Bond Pair

(b) OC Bond Pair

(c) O Lone Pair

(d) O Lone Pair

(e) O Lone Pair (2 equivalent)

(f) O Radical Orbital

Figure 7. Contour plots of the GVB orbitals of CH₃O₂.

The most interesting aspect of the dimethyl peroxide structure is the 180° dihedral angle. The results of our calculations are supported by the photoelectron spectra of Rademacher and Elling.[14] They used the first two ionization potentials to obtain a rough estimate of 170° for this dihedral angle. They obtain 125° for HOOH, suggesting that their estimates are good to 5

(14) P. Rademacher and W. Elling, *Leibigs Ann. Chem.*, 1473 (1979).
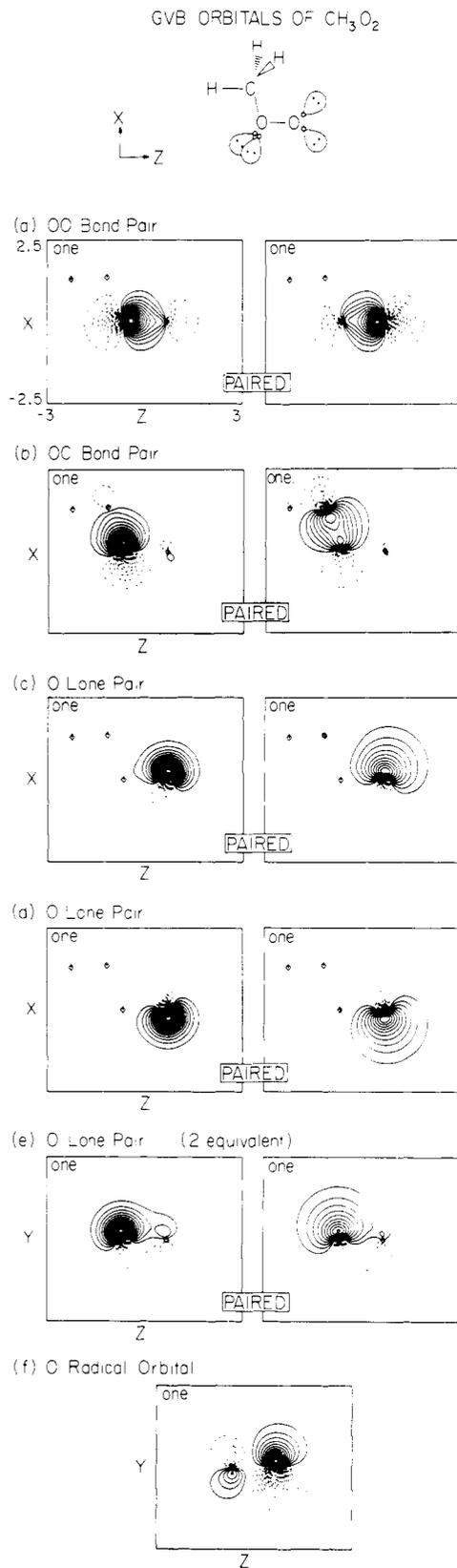
or 10°, and hence their experimental results for CH₃OOCH₃ are consistent with our calculations. Figure 2 shows that the calculated potential curve for the torsional bending of CH₃OOCH₃ is quite flat at the minimum, allowing considerable rotational freedom. It is reasonable that CH₃OOCH₃ be planar since the OH–lone-pair interactions stabilizing the dihedral angle of CH₃OOH and HOOH are absent. The repulsive interactions between CH₃ groups and between CH₃ and lone pairs on different centers favor

Table IV. Calculated Total Energies for GVB + CI Wave Functions of Peroxides and Peroxy Radicals

molecule	energy, hartree	molecule	energy, hartree
HOOH	−151.0216	HOO·	−150.3982
CH₃OOH	−190.0302	CH₃OO·	−189.4090
CH₃OOCH₃	−229.0391		

a 180° dihedral angle (staggered pairs on the two oxygens).

HO₂: The structure of HO₂

$$R_0(\text{OH}) = 0.977 \text{ Å} \qquad R_0(\text{OO}) = 1.335 \text{ Å} \qquad \theta_0(\text{OOH}) = 104.1°$$

is well established, having been obtained from microwave spectra of HO₂ and DO₂ by Beers and Howard.[15] In addition, many theoretical studies have been done on this molecule.[7-9,16-18] Our calculated structure (Table II)

$$R_e(\text{OH}) = 0.972 \text{ Å} \qquad R_e(\text{OO}) = 1.342 \text{ Å} \qquad \theta_e(\text{OOH}) = 104.2°$$

is very close to the experimental one, demonstrating the accuracy of our GVB + CI calculations, which include the resonance terms among the oxygen π orbitals. Of course, we calculate equilibrium

parameters, whereas experimentally, these parameters are measured for the zero quantum level. Thus perfect agreement is not to be expected.

CH₃O₂. This is another case where no experimental data are available, and no previous ab initio calculations could be found. Structurally, CH₃OO is much like HO₂,

$$R_e(\text{CO}) = 1.442 \text{ Å} \qquad R_e(\text{OO}) = 1.339 \text{ Å} \qquad \theta_e(\text{OOC}) = 110.2°$$

The O–O bond lengths are essentially the same, and in both cases the OOR bond angle increases 4–5° from the corresponding peroxide (Table II). The C–O bond length is the same as in the methyl peroxides.

Summary

These calculations are the first reported ab initio studies of the equilibrium structures of CH₃OOH, CH₃OOCH₃, and CH₃OO. The calculated structural parameters of HOOH and HOO are very close to those obtained experimentally, demonstrating the accuracy of the GVB + CI approach.

The dihedral angles of the peroxides are calculated to vary from 119° in HOOH to 126° in CH₃OOH and 180° in CH₃OOCH₃, giving new insight into the gas-phase structures of peroxides.

(15) Y. Beers and C. J. Howard, *J. Chem. Phys.*, **64**, 1541 (1976).
(16) A. Hinchliffe, *J. Mol. Struct.*, **66**, 235 (1980).
(17) T. H. Dunning, Jr., S. P. Walch, and M. M. Goodgame, *J. Chem. Phys.*, in press.
(18) D. H. Liskow, H. F. Schaefer III, and C. F. Bender, *J. Am. Chem. Soc.*, **93**, 6734 (1971).

Electron Nuclear Double Resonance (ENDOR) from Heme and Histidine Nitrogens in Single Crystals of Aquometmyoglobin

Charles P. Scholes,[*1a] **Aviva Lapidot,**[1b] **Rita Mascarenhas,**[1a] **Toshiro Inubushi,**[1c] **Roger A. Isaacson,**[1d] **and George Feher**[1d]

Contribution from the Department of Physics and Center for Biological Macromolecules, State University of New York at Albany, Albany, New York 12222, the Isotope Department, Weizmann Institute of Science, Rehovot, Israel, the Department of Biochemistry and Biophysics, University of Pennsylvania, Philadelphia, Pennsylvania 19174, and the Department of Physics, University of California at San Diego, La Jolla, California 92093. Received July 6, 1981

Abstract: Single-crystal ENDOR studies on the heme and proximal histidine nitrogens were carried out on magnetically dilute crystals of aquometmyoglobin. For some of this work heme nitrogens were enriched to about 90% in ¹⁵N to give simpler ENDOR patterns than the ¹⁴N heme crystals. ENDOR studies were done in three perpendicular planes determined by the heme normal and by the two mutually perpendicular heme nitrogen–nitrogen diagonals. The hyperfine and quadrupole tensors referred to these three directions were obtained for both heme and histidine nitrogens. We found, surprisingly, that diagonally opposite heme nitrogens were electronically not equivalent; i.e., their hyperfine couplings were *not* as expected by four- or twofold symmetry. This inequivalence was most dramatically shown by an approximate 5% difference in ENDOR frequencies within either relevant pair of nitrogens when the magnetic field was along heme nitrogen–nitrogen diagonals. In the orientation pattern near, but not at, the heme normal small variations were seen and were attributed to out-of-planarity of the heme. These variations enabled us to determine that the two nitrogens with larger spin density are on the pyrroles with methyl and propionic acid side chains, while the two nitrogens with smaller spin density are on pyrroles with methyl and vinyl side chains. The hyperfine couplings determined were related via standard ligand field techniques to unpaired electron density in nitrogen 2s and 2p valence orbitals. The primary covalent contributions to the hyperfine interaction arise from nitrogen-to-iron σ bonds. For an average heme nitrogen our analysis gave the percentages of unpaired 2s, 2p_σ and 2p_π electrons as 2.50, 5.6, and 0.9%, while on histidine nitrogen they were 2.92, 7.6, and 0.9%. The quadrupole couplings were analyzed and related to overall electron densities on nitrogen p orbitals. We have used spin Hamiltonian theory to examine the inequivalence of the heme nitrogens with the following results. (1) The measured inequivalence within a pair of heme nitrogens is due to a *real* electronic inequivalence, as opposed to an apparent inequivalence due to second-order effects in the spin Hamiltonian. (2) This real inequivalence arises from the large Fermi contact term in the spin Hamiltonian that is not required by the iron out-of-planarity. (3) The inequivalence can be explained by a small difference (~0.02 Å) in the bond distance to the iron between one heme nitrogen and its diagonally opposite partner.

The goal of this work was to obtain the electronic distribution at heme and histidine nitrogens in aquometmyoglobin. Magnetic

resonance techniques are well suited for this purpose because electron nuclear hyperfine and quadrupole couplings show the